A Study of Ethanol Oxidation in High-Pressure Shock Tube: Ignition Delay Time Measurements and High-speed Imaging of the Ignition Process

D. Nativel, P. Niegemann, J. Herzler, M. Fikri, C. Schulz
Institute for Combustion and Gas Dynamics – Reactive Fluids
University of Duisburg-Essen
Duisburg, Germany

1 Introduction

Non-ideal effects in shock tubes are defined as deviations from the ideal shock-tube reactor assumption. Ideally, the thermodynamic state behind the reflected shock wave is homogeneous and can be calculated from the initial driven gas conditions and the speed of the incident shock wave. However, the development of a sidewall boundary layer [1] causes variations in the thermodynamic state of the compressed test gas [2], which can significantly affect the system and lead to time-dependent changes in temperature and pressure. At higher pressures, a gradual increase in pressure (dp^*/dt) is observed and is often included when simulating ignition [3]. Non-ideal effects have an unneglectable impact on the study of fast chemical processes. In particular, uncertainties in the determination of the rate constants [4] as well as premature ignition (or pre-ignition) at lower temperatures [5] were observed. For the combustion community, understanding pre-ignition has become a major task in the last decade. Among other hydrocarbons, ethanol was found to be prone to have a high pre-ignition tendency [6].

Ethanol is an often-used biofuel and numerous ignition delay time data (IDT) can be found in literature. Zhang et al. [7] gave a detailed comparison of the available ignition delay time data and provided the most updated kinetics mechanism for ethanol oxidation. They also provided results of IDT at 20 bar in a rapid-compression machines (RCM) and a high-pressure shock tube (HPST) for stoichiometric mixtures of ethanol. In 2010, Heufer and Olivier [8] measured IDT of stoichiometric ethanol-air mixtures at pressures and temperature ranging from 13–40 bar and 910–1410 K, respectively. The ignition of ethanol/air mixtures was also investigated in our laboratory in a HPST [9] and results were reported for various nominal pressures (10, 30, and 50 bar) at an equivalence ratio of 1.0 in a temperature range of 800–1250 K. Lee et al. [10] performed ignition delay times measurements in a RCM and a HPST for stoichiometric ethanol/air mixtures at 67–93 bar and 775–1000K. The discrepancy between RCM and shock-tube data increases towards lower temperatures. A direct comparison, however, is not straightforward. This is obvious since the RCM suffers from a long compression phase and heat losses, whereas the shock-tube measurements are influenced by a temperature increase through a continuous pressure rise after the arrival of the reflected shock wave. The

Correspondence to: damien.nativel@uni-due.de

measured data from both facilities are interpreted based on different model assumptions (constant volume with volume profile for the RCM or constant pressure with pressure profile for the shock tube). Lee et al. [10] used schlieren imaging to visualize ignition. They noticed inhomogeneous ignition events leading to a pre-ignition pressure rise. In their literature review, Zhang et al. [7] pointed out a scatter on the available data at low temperature and especially discrepancies between shock tube and RCM data. Recently, a shock-tube study of ethanol oxidation [11] at 2 and 4 bar was reported for equivalence ratios of 0.5 and 1. Additionally, high-speed imaging through a transparent quartz endwall visualized that pre-ignition events are more likely to occur in mixtures containing higher ethanol concentration and that pre-ignition heat release is more pronounced at lower temperatures.

The goal of the present study is to acquire new ignition delay times data in a HPST at high pressure over a domain of temperature where a scatter in measured ignition delay times has been reported in the literature (e.g., at 800–1200 K). Additionally, high-speed imaging using two high-repetition-rate cameras on different positions around the shock tube (endwall and sidewall) provided important information about the ignition process, permitting to distinguish between homogeneous and inhomogeneous ignition in time and space.

2 Experimental Details and Data Acquisition

All the experiments were performed at pressures $p_5 \approx 20$ bar in a HPST. This shock tube has a constant inner diameter of 90 mm and lengths of the driver and driven sections of 6.4 and 6.1 m, respectively, separated by an aluminum diaphragm. The maximum test time can be extended up to 15 ms by driver-gas tailoring using helium and argon. Detailed descriptions of the HPST can be found in a previous publication [12]. The measuring plane of the HPST has four ports to install measuring devices. Figure 1 shows the details of the measuring plane in a cut along the shock tube.

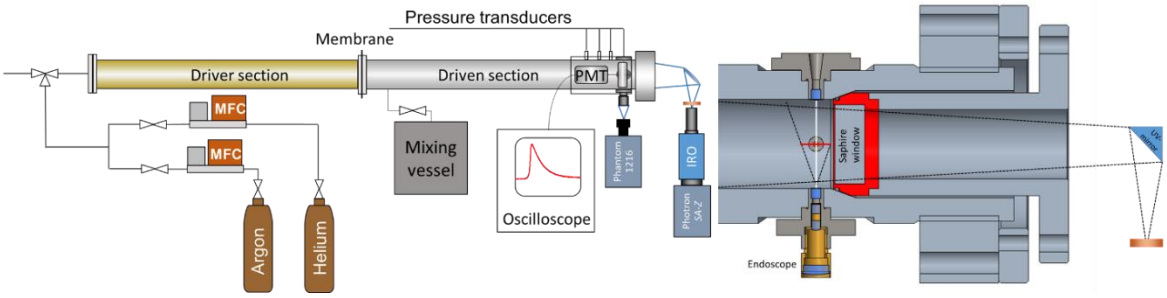

Figure 1. left: Schematics of the HPST; Right: Cut through the measuring plane and the endwall of the shock tube.

In this study, three of the four ports were used. In the top position, a quartz window was mounted in combination with a photomultiplier (Hamamatsu 1P28) that observes spatially-integrated chemiluminescence of OH* through a 310±5 nm bandpass filter). On one side, a UV-transparent endoscope [13] was mounted. This endoscope creates an intermediate image close to the field lens that is recorded by a color high-speed camera (CAM1, Phantom 1216). This camera was equipped with a fast lens (Nikkor 50 mm $f_\# = 1.4$) in combination with a 15-mm spacer ring. The focal plane of the optical system was set to the center of the shock tube illustrated by the red line along the shock-tube axis in figure 1. The third port was used for the fourth pressure transducer (PCB 112A03) while the fourth sidewall port was not used. The endwall consists of a stainless-steel window holder with a 30 mm thick and 80 mm diameter sapphire window. Behind the endwall a 45° UV-enhanced mirror was mounted, hence, the shock tube can be opened without moving the camera system just by removing the mirror and the camera will not be damaged in case the window brakes. The second camera (CAM2, Photron SA-Z equipped with a high-speed intensifier and a UV lens 85 mm $f_\# = 2.8$) detected OH* chemiluminescence via a 2-inch 315±20 nm filter. The focal plane

of this optical system was set to the measuring plane defined by the position of the sidewall windows. Thus, the focal planes of the two camera systems cross in the center of the measuring plane. Both cameras were run at equal frame rate of 30 kHz and 1000–1500 images were recorded. The cameras were triggered by the reflected shock wave detected by the first pressure transducer. High purity ethanol (VWR Chemicals, AnalaR Normapur® ACS, ≥99.8%), oxygen (Air Liquide, 99.998%), and nitrogen (Air Liquide, 99.999%) were used to manometrically prepare the reaction mixtures in a 114-l stainless-steel mixing tank. The mixtures were mechanically mixed with a magnetically-driven stirrer for at least 2 h prior to the experiments. The tank and the HPST were initially heated at 353 K. The HPST was cleaned to remove impurities (particles from membrane or combustion) prior to each experiment. The experiments were carried out in stoichiometric ethanol/air mixtures, one with synthetic air (N_2/O_2 = 3.76) and one with N_2 dilution (N_2/O_2 = 7.62).

3 Results and discussions

Figure 2 shows the measured ignition delay times in comparison to data from literature. At temperatures >950 K, our results agree well with the shock-tube data from Zhang et al. [7], Heufer et al. [8], and Cancino et al. [9]. At lower temperatures, a large discrepancy between the RCM data at 20 bar from Zhang et al. [7] and shock tube data from literature and this study is noticed. Our results agree with those from Heufer et al. [8] and Cancino et al. [9] over the whole temperature range.

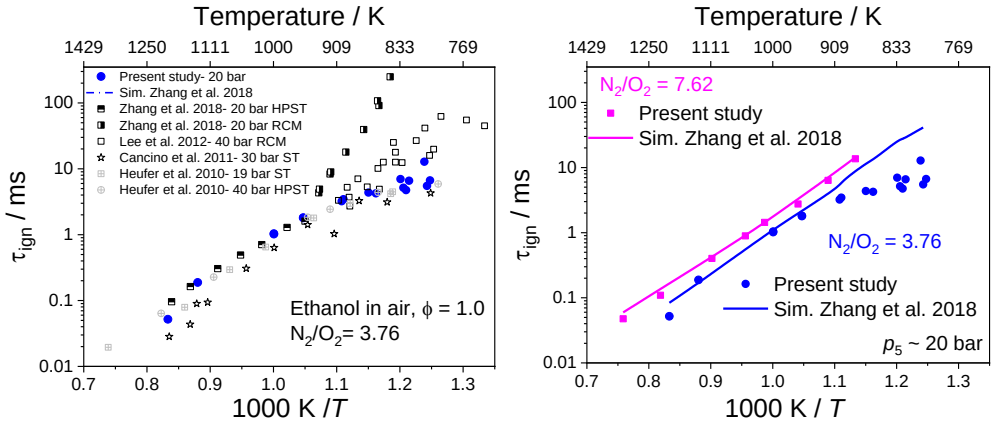

Figure 2. Ignition delay times of stoichiometric ethanol/air mixtures. Left: Comparison between experimental results and literature; right: Comparison between experiments and simulation from Zhang et al. [7].

The difference between RCM and shock-tube data is mostly due to pre-ignition and was clearly noticed on the pressure profiles (see figure 3). For the lowest temperature, the determination of the ignition delay was more difficult than at high temperature since only a weak pressure increase was observed. Thus, the OH* emission profiles were used for the low-temperature range (800–900 K). Figure 2 shows a comparison between N_2-diluted and non-diluted stoichiometric ethanol/air mixtures and also with the simulation results based on the Zhang et al. [7] mechanism. The simulations were performed with Chemical Workbench [14] using a "specified-pressure" reactor model with the possibility to implement an experimental dp*/dt. Thus, for each experiment a dp*/dt was determined and used for simulation. The simulations agree very well with the results for the N_2-diluted mixtures but deviate for the non-diluted mixtures below 950 K.

Sidewall and endwall high-repetition-rate imaging were obtained for the non-diluted mixture whereas only sidewall imaging using the colored camera were captured for the N_2-diluted one. The agreement between experiment and simulation observed in figure 2 for the diluted mixture gives confidence about the existence

of a quasi-homogenous ignition. Figure 3 shows that for the diluted mixture there is almost no pre-ignition detected from the pressure traces at comparable reaction times. As mentioned in section 2, a driver-gas tailoring method was employed to extend the test time. Nevertheless, we notice in figure 3 that for some shocks (e.g.: 807 K, 918 K) the tailoring was not perfect inducing a small decrease of pressure (too much helium in the mixture He-Ar).

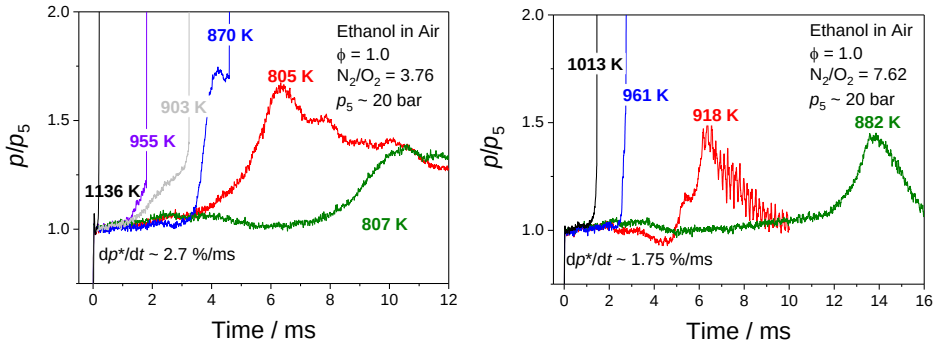

Figure 3. Temporal evolution of the post-shock reflected pressure. Left: Non-diluted stoichiometric mixture ($N_2/O_2 = 3.76$); right: N_2-diluted stoichiometric mixture ($N_2/O_2 = 7.62$).

For the non-diluted mixture, homogenous ignition was observed above 950 K, while at lower temperatures, pre-ignition becomes significant. Below 950 K, many scenarios of inhomogeneous ignition were observed. We selected three cases (Case 1: T_5 = 807 K; Case 2: T_5 = 805 K and Case 3: T_5 = 870 K) shown in figure 3 but with more details in figures 4 and 5. Figure 4 shows the cases 1 and 2.

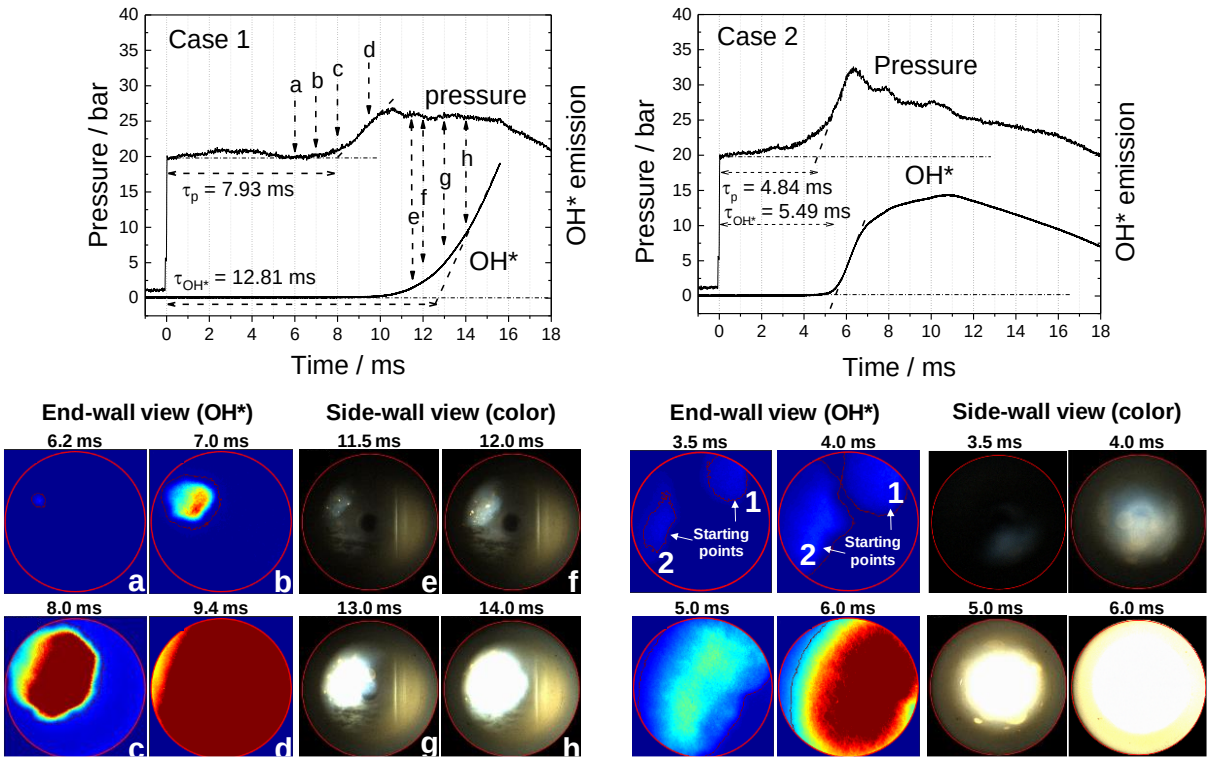

Figure 4: Luminescence images for the non-dilute ethanol/air mixture at initial post-shock conditions of ~800 K and 20 bar. Left: Ignition not localized at the endwall; right: Ignition localized near to the endwall.

These experiments were performed with exactly the same initial conditions but exhibit two completely different behaviors. For case 1, the IDT determined from the OH* signal measured through the sidewall is 12.81 ms and for the case 2, 5.49 ms. In both cases, the pressure increases at earlier times than the OH* signal (especially case 1). This could be explained by ignition further away from the end flange, which apparently produces pressure waves leading to pressure increase in the measurement plane without appearance of emission. Using the two-camera high-speed imaging setup, we could localize the origin of the ignition which is not possible to detect using a single camera system due to the limited depth resolution. The two runs manifest two different ignition processes, far from the endwall for the longest delay (case 1) and an ignition near to the endwall for the lowest delay (case 2). For case 1, the endwall OH* camera showed a first ignition in an off-center position at around 6 ms (frame a) that propagated and fully covered the shock-tube cross-section at around 10 ms (d). Consequently, a compression wave is generated and increases the pressure in the shock tube. After 10 ms, the sidewall color camera observed the arrival of the propagating flame (e) and a weak ignition at around 13–14 ms (g and h). Simultaneously, the OH* photo-multiplier signal rises once the flame reaches the measurement plane. A significantly different ignition mode is observed for case 2 with a good agreement of the observations of the two cameras. The endwall camera showed two independent starting points of the ignition. In a similar study, Figueroa-Labastida et al. [11] came to the conclusion that low-temperature ignition is initiated from individual hot spots.

Figure 5 shows an example of ignition from two simultaneous views of the shock tube that is apparently initiated and driven by a hot particle, presumably a fragment of the diaphragm. At t_1, we can observe a yellow spot that is characteristic for diaphragm particles through the sidewall window while from the endwall camera nothing can be observed (the glowing particle does not emit in the UV). At t_2, the fuel surrounding the particle starts to ignite, which is seen in the sidewall as well as in the endwall view (right side of the bottom frame 2). Based on these observations together with the late frames (highest OH* emission around the particle at t_5, t_6) it is obvious that the main ignition occurs near the endwall where the hot particle initiates a flame kernel.

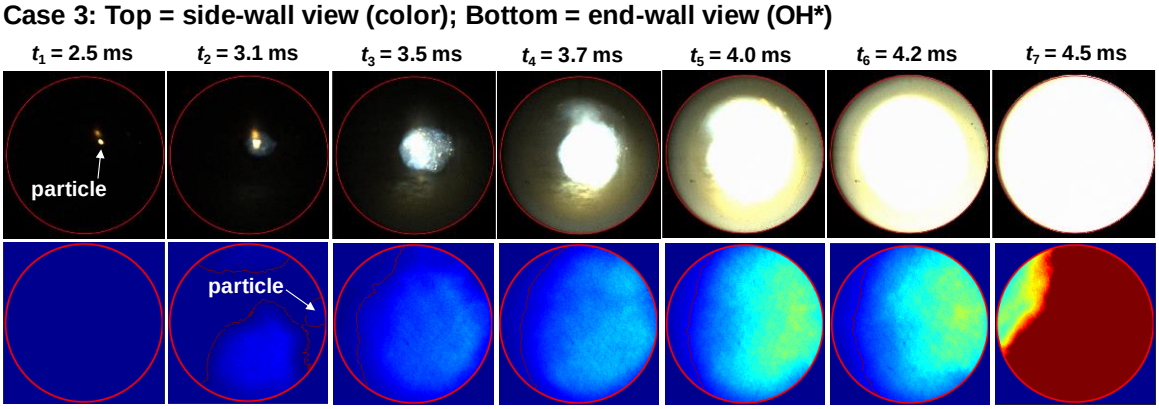

Figure 5. Sequence of images of an inhomogeneous ignition event of the non-diluted ethanol/air mixture at initial post-shock conditions of ~870 K and 20 bar presumably initiated by a hot particle.

4 Conclusions and future work

New ignition delay times were measured for N_2-diluted and non-diluted stoichiometric ethanol/air mixtures at ~20 bar from 800 to 1250 K. The results were compared to literature data. Good agreement was observed for the high-temperature results with the data from Zhang et al. [7], Heufer et al. [8], and Cancino et al. [9]. At lower temperatures, a considerable discrepancy was noticed between RCM data from Zhang et al. [7]

and all shock-tube results, including those from literature. The ignition phenomena corresponding to our experimental results were simulated using the kinetics model of Zhang et al. [7]. Very good agreement was found for the diluted mixture and a deviation was observed at lower temperature for the non-diluted mixture.

To further investigate the ignition, simultaneous high-speed imaging was performed for two viewing directions. In general, we noticed homogeneous ignition for the diluted mixtures. For the non-diluted mixtures, the presence of different non-homogenous ignition modes was recognized. We could observe ignition far or near from the endwall for the nominally identical experimental conditions and also for some cases ignition initiated by a hot (potentially burning) fragment of the diaphragm.

Acknowledgments

This work is supported by the German Research Foundation within the DFG Project SCHU 1369/27.

References

[1] Davidson DF, Hanson RK. (2009). Recent advances in shock tube/laser diagnostic methods for improved chemical kinetics measurements. Shock Waves 19: 271.

[2] Mirels H. (1972). Boundary layer growth effects in shock tubes. Proc. 8th Int. Shock Wave Symp. 2-30.

[3] Pang GA, Davidson DF, Hanson RK. (2009). Experimental study and modeling of shock tube ignition delay times for hydrogen–oxygen–argon mixtures at low temperatures. Proc. Combust. Inst. 32: 181.

[4] Petersen EL, Hanson RK. (2001). Non-ideal effects behind reflected shock waves in a high-pressure shock tube. Shock Waves 10: 405.

[5] Petersen EL et al. (2009) Discrepancies between shock tube and rapid compression machine ignition at low temperatures and high pressures. In: Hannemann K., Seiler F. (eds) Shock Waves. Springer, Berlin, Heidelberg.

[6] Hamilton L, Caton P, Cowart J. (2008). Pre-ignition characteristics of ethanol and E85 in a spark ignition engine. SAE paper 2008-01-0321.

[7] Zhang Y, El-Merhubi H, Lefort B, Le Moyne L, Curran HJ, Kéromnès A. (2018). Probing the low-temperature chemistry of ethanol via the addition of dimethyl ether. Combust. Flame. 190: 74.

[8] Heufer KA, Olivier H. (2010). Determination of ignition delay times of different hydrocarbons in a new high pressure shock tube. Shock Waves. 20: 307.

[9] Cancino LR, Fikri M, Oliveira AAM, Schulz C. (2011). Ignition delay times of ethanol-containing multi-component gasoline surrogates: Shock-tube experiments and detailed modeling. Fuel 90: 1238.

[10] Lee C, Vranckx S, Heufer KA, Khomik SV, Uygun Y, Olivier H, Fernandez RX. (2012). On the chemical kinetics of ethanol oxidation: shock tube, rapid compression machine and detailed modeling study. Z. Phys. Chem. 226: 1.

[11] Figueroa-Labastida M, Badra J, Elbaz AM, Farooq A. (2018). Shock tube study of ethanol preignition. Combust. Flame. 198: 176.

[12] Niegemann P, Fikri M, Wlokas I, Röder M, Schulz C. (2018) Methodology for the investigation of ignition near hot surfaces in a high-pressure shock tube. Rev. Sci. Instrum. 89: 055111.

[13] Reichlet R, Pruss C, Gessenhardt C, Schulz C, Osten W. (2012). Diffractive/refractive (hybrid) UV-imaging system for minimally invasive metrology: design, performance, and application experiments. Appl. Opt. 51: 1982.

[14] Deminsky M, Chorkov V, Belov G, Cheshigin I, Knizhnik A, Shulakova E, Shulakov M, Iskandarova I, Alexandrov V, Petrusev A, Kirillov I, Strelkova M, Umanski S, Potapkin B. (2003). Chemical Workbench - integrated environment for materials science. Comp. Mater. Sci. 28: 169.